The International Journal of Advanced Manufacturing Technology (2019) 102:4257–4271
https://doi.org/10.1007/s00170-019-03291-3

ORIGINAL ARTICLE

High speed machining of near-beta titanium Ti-5553 alloy under various cooling and lubrication conditions

Emre Tascioglu[1] · Armin Gharibi[1] · Yusuf Kaynak[1]

Received: 9 October 2018 / Accepted: 2 January 2019 / Published online: 8 March 2019

Abstract
Extreme tool wear resulting in short tool life is one of the main issues in the cutting process of near-beta Ti alloys. This study provides extensive experimental results and new findings that help to understanding progressive tool wear and the corresponding measures in high speed machining of Ti-5553 alloy under various coolant and lubrication (dry, flood, high-pressure coolant, MQL, and Cryogenic cooling) conditions at finish and semi-finish cutting. Cutting temperature, progressions of tool wear, and tool life are presented. Besides, cutting forces, frictional conditions, and chip morphology are studied. This current work provides evidence that supports the argument that the feasibility of high speed machining of near-beta titanium alloys that depends on cutting conditions, namely coolant and lubrication used during machining. It was found that tool wear is developed by an abrasive and adhesive mechanism, and built-up-edge formation is a common problem in the machining of this alloy. A high pressure coolant supply with its cooling and lubrication ability was found to be very helpful for decreasing the coefficient of friction and temperature during the process, consequently lowering progression of wear and cutting force components when compared to other cooling and lubrication conditions tested in this study. The greatest tool life is achieved by high-pressure coolant supply, and cryogenic cooling achieves the second greatest tool life. Minimum quantity lubrication is found to be inefficient for improving the machining performance of this alloy. Finally, it is found that the selected depth of cut has vital effect on the penetration capability of cooling and lubrication in between tool and chip, and consequently, it plays a significant role in the contribution of cooling and lubrication to the machining performance of this alloy.

Keywords Tool life · Progressive tool wear · Machining performance · Titanium alloys

1 Introduction

Titanium alloys are widely preferred in various industries because of their perfect combination of strength-to-weight ratio even at elevated temperature [1–3]. While they have such exceptional properties, they have some additional aspects such as low conductivity, high chemical reactivity, and low modulus of elasticity that leads to difficulties occurring in forming these alloys in plastic deformation processes particularly in a machining process [1, 2, 4–6]. Because of these properties, cutting tools are subjected to various wear mechanisms during the machining process of titanium alloys, and consequently, tool life becomes short. Furthermore, other properties such as low Young's modulus leads to reducing the machining performance of these materials [7]. Unstable chip breakability is another problem in the machining of titanium alloys which causes low surface quality and fractures on cutting inserts due to chip hammering [8]. All these problems increases the manufacturing cost of the components made of titanium alloys [9].

There are many strategies to improve the machinability and thus to reduce the manufacturing cost, such as enhancing the effectiveness of the machining, improving insert materials, effective programming of the machining center, improving the tool life via machining condition strategies, and decreasing the energy by implementing lubrication or heating the work material [10–12], but among these solutions, using cooling and lubrication strategies attracts more attention. Improving the machining performance of such alloys has been achieved through using high-pressure coolant (HPC), minimum quantity lubrication (MQL), and application of cryogenic cooling [13–18]. Many studies reported that utilizing cryogenic coolant and high-pressure coolant is helpful to eliminate/reduce

✉ Emre Tascioglu
emre_tascioglu@hotmail.com

[1] Department of Mechanical Engineering, Technology Faculty, Marmara University, Goztepe Campus, Kadikoy, 34722 Istanbul, Turkey

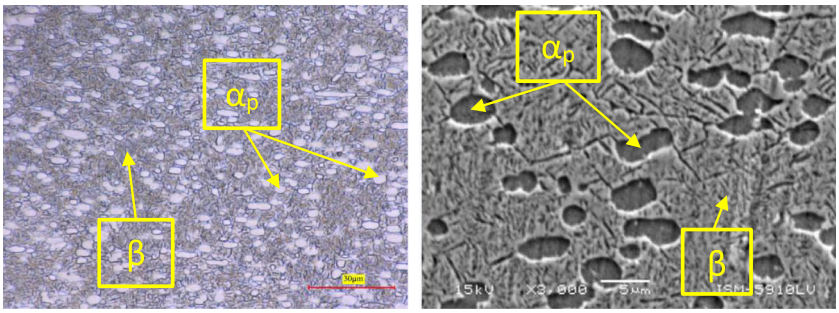

Fig. 1 Microstructural image workpiece (Ti-5Al-5V-5Mo-3Cr): **a** OM image and **b** SEM [23]

the aforementioned difficulties in the machining of Ti-6Al-4V alloy [9, 17, 19, 20]. Limited studies reported the examination of the influence of the coolant and lubrication on the machinability of near-beta alloys in particular Ti-5553 alloy [21–24]. These studies underlined that near-beta Ti-5553 alloy has much superior properties, such as high yielding stress, and endurance, and consequently, it has much lower machining performance compared with Ti-6Al-4V alloy [22]. When machining this near-beta alloy, much lower cutting speed is preferred, but tool life is still much shorter in machining this alloy compared with Ti-6Al-4V [25]. Our recent study showed that HPC provides obvious benefit for reducing tool wear, force components, and chip thickness. Furthermore, HPC also improved the surface integrity compared with flood cooling and MQL [24]. Although the role of high-pressure coolant supply for the single pass at constant depth of cut is presented in that paper, the tool life and the machining performance from the beginning of cutting till the end of tool life is missing in that paper [24].

This study provides a comprehensive study by focusing on the machining of Ti-5553 alloy under different cooling and lubrication strategies by examining tool life under two different cutting speeds and two different depths of cut considering finish and semi-finish cutting. Besides, changes of forces, temperature, and chip morphology with the progression of tool wear are also investigated.

2 Experimental details

The workpiece was near-beta titanium Ti-5Al-5V-5Mo-3Cr alloy. A 20 mm round bar in hot-rolled condition with average 317 ± 5 HV hardness was used in all machining trials. Thermal conductivity for this alloy is 8.6 W/m °C [26]. It has bimodal microstructure (BM) [27] by including α and β phases [11]. It also includes α_p (primary α phase) particles [27], as shown in Fig. 1. It was reported in various references the beta transus is at around 845–850 °C for this material [28, 29].

The cutting tool, tool holder, and the details of the machining center used in cutting tests are presented in Table 1. The details of the selected cutting parameters and conditions of machining are presented in Table 2. The selected cutting speeds were 90 and 120 m/min. The 90 m/min cutting speed was also used by Braham-Bouchnak et al. [21] in the machining process of Ti-5553 alloy. The 120 m/min cutting speed was chosen considering the studies on the machining of Ti-6Al-4V [30]. Experimental setup is presented in Fig. 2.

A Piezoelectric KISTLER 2129AA dynamometer was used to record forces. A Keyence digital optical microscope was used for measuring tool wear and chip morphology. An Optris PI 400 camera was used to record the cutting temperature. All the details of temperature measurement of this particular work material for various temperature ranges are presented elsewhere [23]. Considering the wide range of temperature including low cryogenic temperature, 0.63 is used as an emissivity [31]. An example of the measured temperature profile is shown in Fig. 3.

3 Results and discussion

3.1 Machining performance

3.1.1 Cutting temperature

Compared with many engineering materials, high temperature is the main concern in the machining process of Ti-based materials because of their much lower thermal conductivity. Eventually, heat builds up at the tool-chip interface, substantially affecting the cutting operation [32]. The temperature during the machining process needs to be measured to interpret the progression of wear in the machining process, especially for titanium alloys. This is important if the cutting temperature can reach, or approach close, to the softening temperature of the cutting tool, such that it loses hardness. In such

Table 1 Experimental conditions

Cutting tool	883 Grade Carbide insert, CNMG120408-M1
Tool holder	PTJNL2525M16JET
CNC center	DOOSAN CNC turning center, 18 KW, 4500 RPM

Table 2 Cutting parameters and cooling conditions

Cutting speed, V_c (m/min)	Cutting conditions	Depth of cut, a_p (mm)	Feed rate, f (mm/rev)
90	Dry (no cooling and lubrication)	0.6 (Finishing)	0.15
120	Cryogenic (LN_2 assisted, 15 bar; 10 g/s mass flow)	1.2 (Rough)	
	MQL (21 ml/h; 0.4 MPa)		
	HPC (50 bar), XTREME CUT		
	Flood (400 l/h)		

cases, the progression of wear is expected to accelerate, and in a short time the cutting tool can reach the end of its life. Due to the experimental setup measuring the exact value of the maximum temperature occuring in between the cutting tool and chip in the turning process includes challenges. Instead, the maximum temperature that occuring in the cutting region from the top of the newly generated chip was measured. Temperature measurement during the experimental study is schematically shown in Fig. 4.

The recorded maximum temperatures are approximately 566 °C, 530 °C, and 267 °C in dry, MQL, and cryogenic conditions, respectively, at the beginning of the machining process when $a_p = 1.2$ mm and $V_c = 120$ m/min (Fig. 4). Increased length of machining results in increased temperature as expected due to rapidly increased wear. At the end of the cutting process, the temperature values measured were 862 °C, 764 °C, and 389 °C in dry, MQL, and cryogenic cutting, respectively. It is seen that dry and MQL machining produce temperatures close to each other. Besides, cryogenic cooling makes a notable difference by generating less temperature in the machining operation. Although these trends were already observed in the cryogenic machining process of various alloys [33] including titanium alloys [9, 34], the contribution of this current study is to confirm this trend in machining near-beta alloys (Fig. 5).

A similar trend is also observed with finish machining as depicted in Fig. 6. The temperature rises rapidly in dry and MQL conditions as the cutting distance increases. The cutting temperature shows up to 36% increase from 412 to 561 °C in dry cutting condition and 32% increases from 412 to 544 °C in MQL cutting condition. However, the measured cutting temperature is approximately between 200 and 300 °C under cryogenic condition. As the growth of tool wear increases with respect to the cutting length, the rake and clearance surface of the cutting tool become discontinuous, which might help liquid nitrogen to further penetrate towards the tool tip. This slightly reduces the cutting temperature, although flank

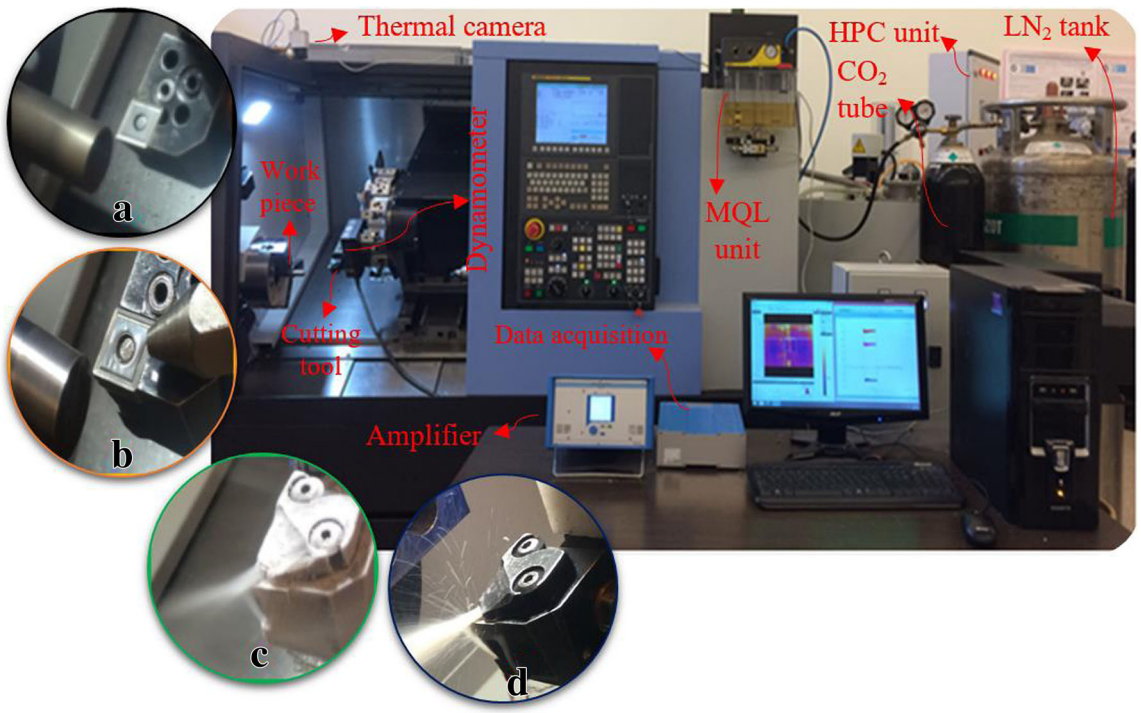

Fig. 2 Experimental setup: **a** dry, **b** MQL, **c** applying liquid nitrogen (cryogenic), and **d** HPC

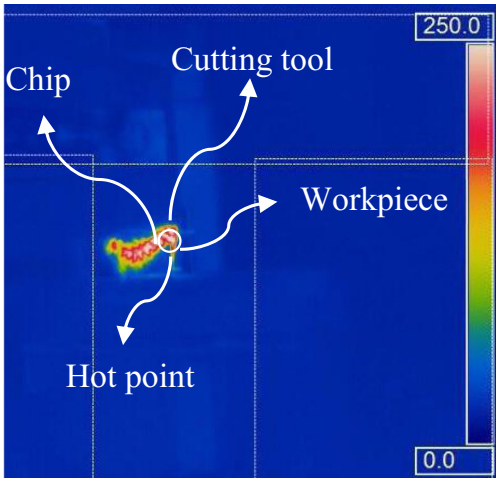

Fig. 3 Example of measured temperature profile

and nose wear keep increasing. Smaller depth of cut results in notably decreased temperature in dry and MQL conditions. Consequently, the depth of cut plays a critical role in raising temperature in machining this alloy, and this argument can be supported by the evidence depicted in Fig. 7.

The available model is also utilized to predict temperature rise in the machining of Ti-5553 alloy. The empirical method developed by Nathan Cook [35] was used to calculate the cutting temperature, and the results were compared with experimental measurements.

$$T_r = \frac{0.4U}{\rho C}\left(\frac{Vt_0}{K}\right)^{0.333} \tag{1}$$

where T_r is interface temperature, U is specific energy, V is cutting speed, t_o is depth of cut, ρC is volumetric specific heat of work material; and K is thermal diffusivity of workpiece, calculated from:

$$K = \frac{k_t}{\rho C} \tag{2}$$

where k_t is thermal conductivity of workpiece. Cutting temperature is calculated considering the following:

$$T = T_0 + T_r \tag{3}$$

where T is cutting temperature and T_0 is room temperature. Figure 8 shows the calculated temperature and measured temperatures at 120 m/min in different machining conditions. The difference between calculated and measured values is approximately 22%. This difference is acceptable considering the recording region of temperature and the region where expected maximum temperature is observed.

3.2 Tool wear and life

Figure 9 shows the measured maximum flank wear of cutting tools utilized in different cooling and lubrication during

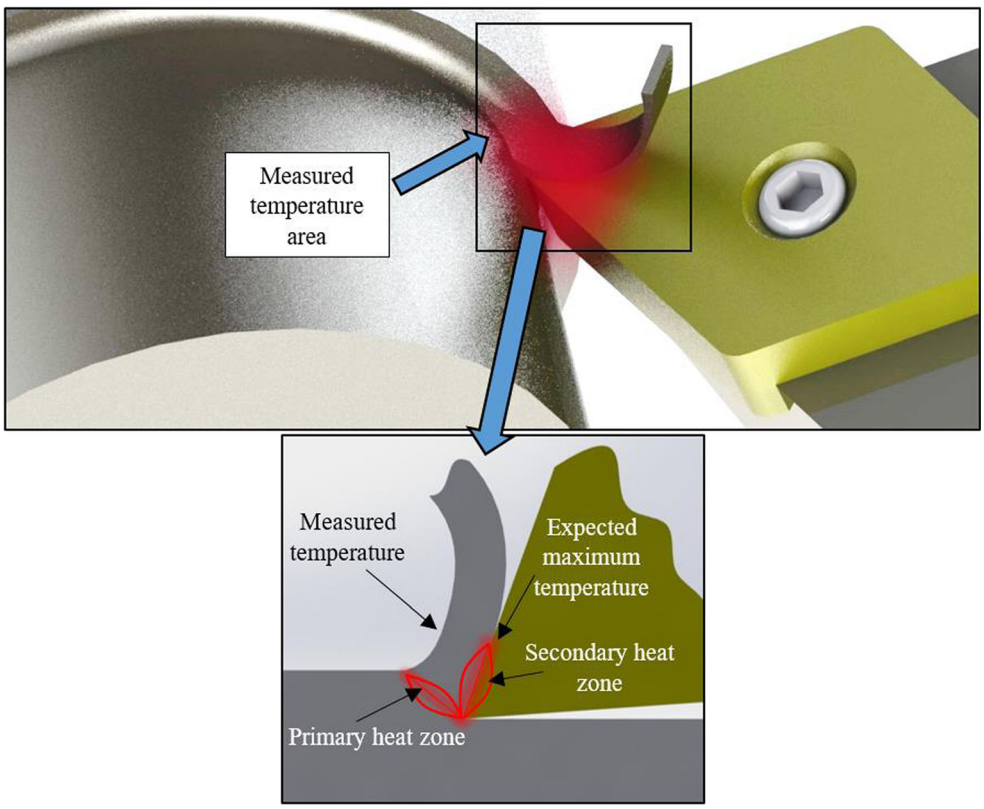

Fig. 4 Schematic diagram of the temperature measurement

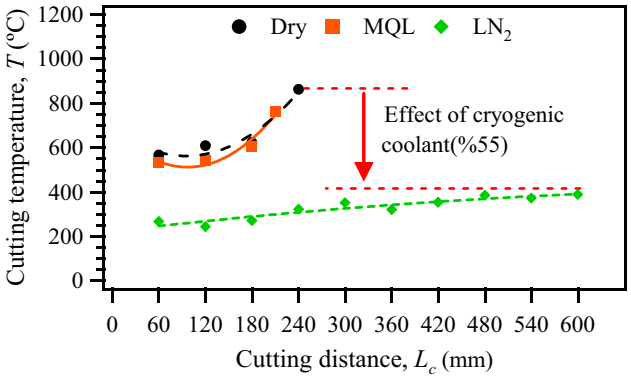

Fig. 5 Measured cutting temperature under various machining conditions (a_p = 1.2 mm. V_c = 120 m/min)

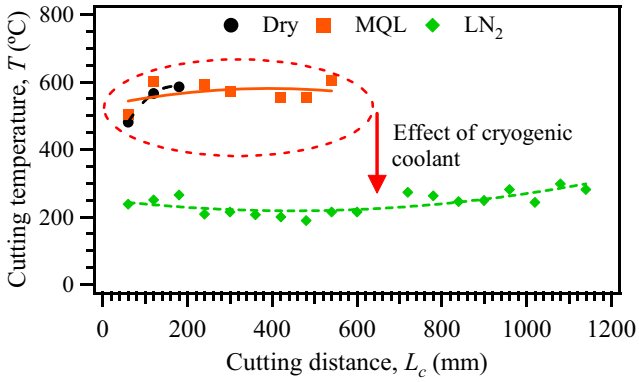

Fig. 7 Measured cutting temperature under various machining conditions (a_p = 1.2 mm. V_c = 90 m/min)

machining of work material. A notable influence of various cutting conditions on the progression of tool wear and eventually tool life is observed, as shown in Fig. 9. While the trends of progression of wear in dry, MQL, and flood cooling are close to each other with respect to cutting length, liquid nitrogen and high-pressure coolant supply shows remarkable difference. Considering ISO 3685:1993, it is assumed that the cutting insert reaches the end of its life when the length VB_{max} reaches 600-μm when the depth of cut is 1.2 mm and 300-μm when the depth of cut is 0.6 mm. While in dry, flood, and MQL conditions, tools can no longer be used after 180-mm cutting length, it is 540 mm in cryogenic machining and the length of cut is 1300 mm in HPC conditions. Lowering cutting speeds by keeping the depth of cut constant is beneficial to increase tool life, but the role of cooling and lubricant to determine tool performance does not show a notable difference, as depicted in Fig. 10.

In finish machining (Fig. 11), the observed trend shows some changes taking the effects of cooling and lubrication into account when compared with the data obtained with larger a_p. The notable difference is that MQL and flood conditions shows much better performance, and cryogenic cooling is very effective when compared to its effect in larger depth of cut conditions, as presented in Fig. 9. It is found that the depth of cut has a substantial effect on the cooling and lubrication role to determine tool life. Furthermore, dry machining of this alloy even in finish operations seems to be not feasible as the tool is worn out sharply because of the relatively low softening point temperature of the carbide tool, approximately 1100 °C [36]. Indeed, the recorded temperature does not reach this level. However, the hardness of the cemented carbide tool is seriously impacted by the elevated temperature. Its hardness decreases more than 50% at around 800 °C, compared with the hardness of the carbide tool at the room temperature [36]. Thus, the cutting tools loses its resistance and consequently reaches the end of life in a short time in dry and MQL conditions as well.

Chip hammering takes place in dry, MQL, and cryogenic conditions, but it was not observed in HPC condition

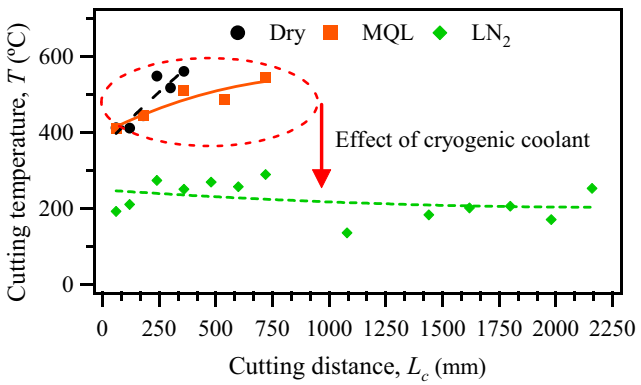

Fig. 6 Measured cutting temperature under various machining conditions (a_p = 0.6 mm. V_c = 120 m/min)

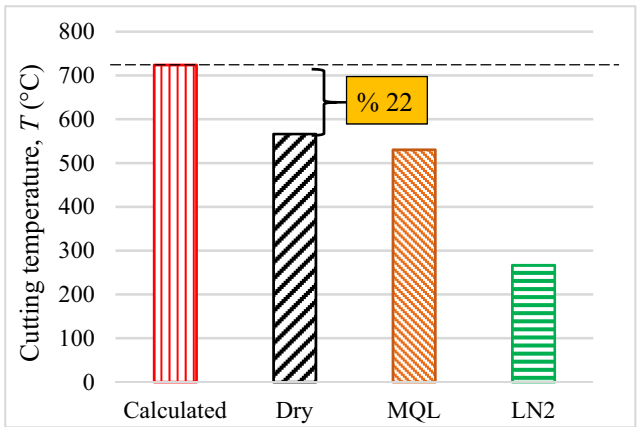

Fig. 8 Predicted and measured temperatures in different cutting conditions

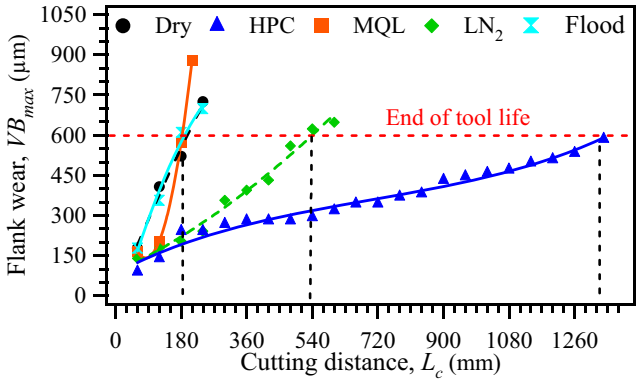

Fig. 9 Flank wear variation with respect to cutting length (a_p = 1.2 mm, V_c = 120 m/min)

(Fig. 12). Chip hammering takes place because of the high friction and large contact length during its flow toward the major cutting edge on the rake face [37]. As schematically illustrated in Fig. 13, during chip side flow, it damages the cutting edge. While extreme damage is observed in dry and MQL conditions. Liquid nitrogen (LN_2) also results in reduced damage on the cutting edge. It was also reported in the literature that cryogenic cooling, including CO_2 [38] and LN_2 [37], reduces chip flow damage, which supports the results presented here. However, HPC completely eliminated this problem as it generated very short and tubular chips, as shown in Fig. 14.

Built-up edge formation is a commonly observed problem in cutting of this alloy, as illustrated in optical microcopy images in Figs. 11 and 15. Recorded temperature are very high in dry and MQL conditions, which consequently softens work material. Germain et al. [39] carried out mechanical tests for this particular material under various temperatures. They reported that increasing workpiece temperature leads to decreased yield and ultimate tensile stress of it and also increased

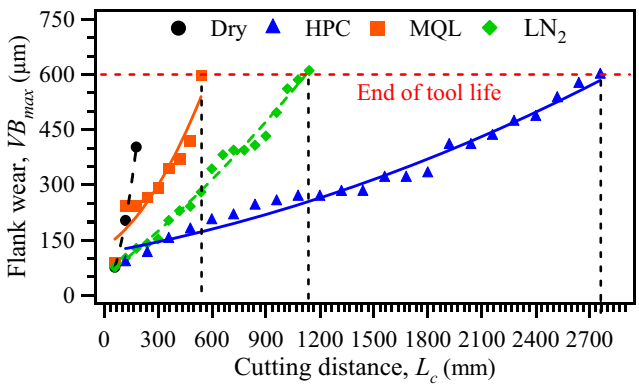

Fig. 10 Flank wear variation with respect to cutting length (a_p = 1.2 mm, V_c = 90 m/min)

ductility, as shown in Fig. 16. As a result, there is a tendency of the workpiece to adhere to the edge of the tool, and eventually built-up edge formation throughout the cutting edge at the nose region takes place. Similar results were reported in the literature [26, 40]. Furthermore, wear is developed by the adhesion mechanism that can be observed on the nose region of cutting tools and also on the worn surface of the flank area as shown in Fig. 15. Another dominating wear mechanism on the clearance face of the insert is abrasion. Grooves parallel to each other on the worn area are good indicators of this mechanism. All these wear mechanisms leads to wear developing quickly in dry and MQL machining. Although these wear mechanisms are also observed in HPC and cryogenic cooling conditions, cooling and lubrication seem to suppress the progression of wear by effectively cooling and lubricating the cutting area.

Tool life as a function of various coolant and lubrications is one of the outputs of this study. Figure 17 shows that tool life in HPC cooling condition is approximately 4 min. In LN_2 conditions, tool life is 1.6 min. MQL, dry, and flood cooling lead to more or less similar performance, and in these conditions, tool life is less than a minute at 120 m/min when a_p = 1.2 mm. It is obvious that reaching the end of tool life is strongly dependent on cooling and lubricating conditions. However, cutting parameters also play a vital role to determine the life of the insert. For instance, when V_c is decreased to 90 m/min at same depth of cut value, tool life becomes almost 12 min. In HPC condition, that is a very reasonable and acceptable tool life when compared to tool life recorded at 120 m/min. A similar increase in tool life is observed in all other cooling and lubrication conditions when cutting speed is lowered from 120 to 90 m/min. When HPC condition is taken as a reference, reducing cutting speed from 120 to 90 m/min resulted in a 180% increase in the life of the cutting tool. In cryogenic machining, the increase is approximately 193%. In addition to cutting speed, it is obvious that the depth of cut also plays a remarkable role in improving the performance of the cutting tool. When it is reduced from 1.2 to 0.6 mm, tool life showed a 104% increase in HPC coolant conditions. More interesting results are obtained with cryogenic cooling when the depth of cut is changed. The tool life shows a 318% increase when a_p is decreased from 1.2 to 0.6 mm in cryogenic cooling condition. Except for dry condition, reduced depth of cut helped to increase tool life in all four conditions.

Having the approximate tool life for various cutting speeds might be useful for industrial application. Thus, the well-known Taylor tool life equation [41], shown below, was used to predict tool life for two different cutting speeds.

$$V_c.T^n = C \tag{4}$$

where V_c is cutting speed, T is life, and n and C are constants.

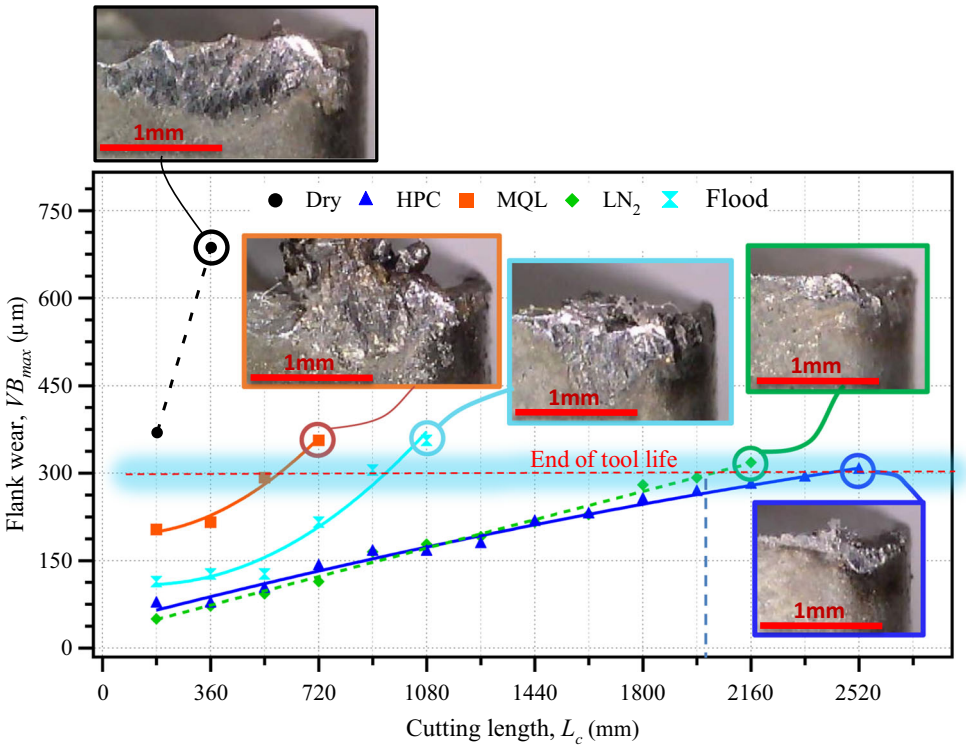

Fig. 11 Flank wear variation with respect to cutting length (a_p = 0.6 mm, V_c = 120 m/min)

The predicted tool life based on the Taylor tool life equation for HPC and cryogenic conditions is presented in Fig. 18.

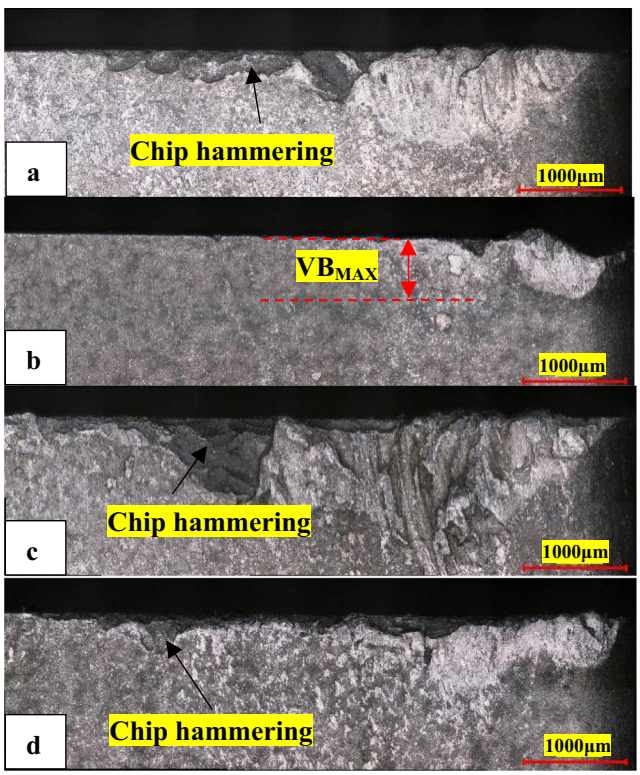

Fig. 12 Images of flank wear: **a** dry, **b** HPC, **c** MQL, and **d** LN_2 (a_p = 1.2 mm, V_c = 90 m/min)

When V_c is decreased from 90 to 60 m/min, tool life shows a 320% increase and becomes 50 min in HPC condition. But, when increasing cutting speed to 150 m/min, tool life becomes less than 2 min. Tool life can become approximately 22 min when the cutting speed is selected as 60 m/min in cryogenic cooling conditions. Among all cooling and lubrication conditions, HPC conditions show the most promising results in terms of reducing the progression of tool wear and remarkably extending tool life in the cutting process of Ti-5553 alloy. Utilizing liquid nitrogen in the cutting process at a particularly smaller depth of cut also provides some advantages compared with flood cooling and MQL machining.

3.3 Forces and friction

Three components of force, namely F_x, F_y, and F_z, were considered, and the resulting force was calculated utilizing following well-known equation.

$$F_r = \sqrt{F_x^2 + F_y^2 + F_z^2} \tag{5}$$

The obtained results are illustrated in Figs. 19 and 20 considering 1.2 and 0.6-mm depth of cut, respectively. It is apparent that the resulting forces are noticeably affected by the progression of tool wear. These resulting forces exhibit similar trends with the progress of flank wear. The smallest resulting forces were recorded in HPC conditions, among all five

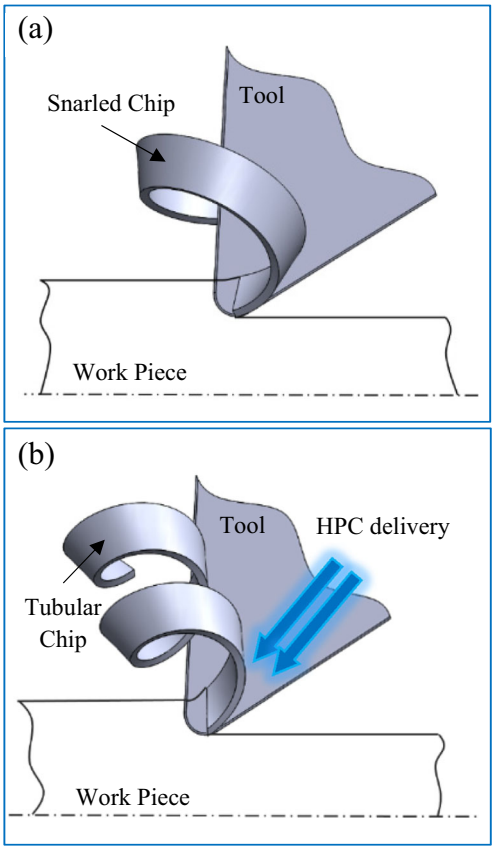

Fig. 13 Schematic diagram of chip side flow: **a** dry and **b** HPC

conditions. The change of the resulting force from the beginning of the cutting process until the end of tool's life is also presented in the same figure. The largest variation is recorded in MQL condition. However, the smallest variation is recorded in HPC condition as 36.2%. In case of LN_2 condition, the resulting force leads to a 64.4% increase during the progression of wear, which is also much lower than that of dry, MQL, and flood cooling conditions.

Figure 19 shows the variation of the resulting force as a function of cutting length in finish machining. Similar to larger depth of cut results, the resulting force in HPC condition exhibits the smallest force among all five conditions. Another important point that needs to be underlined is that the resulting forces recorded in dry machining during the first 360 mm cutting length is much larger than the resulting force recorded during other cutting conditions. Cryogenic and flood cooling also display a tendency for a large increase in the resulting force with increasing cutting length, which indicates that tool wear dominated the trend of the resulting force in the machining process of this alloy.

The coefficient of friction (μ) [9, 42] between the chip and cutting tool is calculated by the following equation:

$$\mu = \frac{F_C \, sin\alpha + F_N \, cos\alpha}{F_C Cos\alpha + F_N \, sin\alpha} \tag{6}$$

where F_c is the main cutting force, α is the tool rake angle, and F_N is the force normal to the tool flank face. In this case, it is 93°. Hence, F_N can be given as [9, 42]

$$F_N = \left| F_r \, sin\theta - F_f \, cos\theta \right| \tag{7}$$

where F_r is the radial force, F_f is the feed force, and $\theta = 3$. The calculated results for the coefficient of friction are shown in Table 3. A large difference between the first pass and second pass in terms of coefficient of friction is obtained in all conditions. The largest variation between the first pass

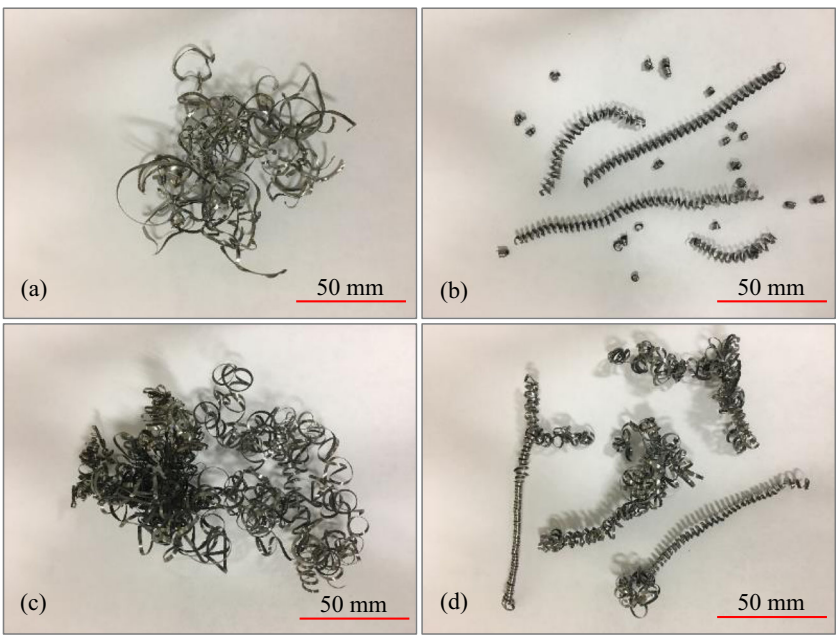

Fig. 14 Generated chips under various machining conditions: **a** dry, **b** HPC, **c** MQL, and **d** LN_2 ($a_p = 1.2$ mm, $V_c = 90$ m/min)

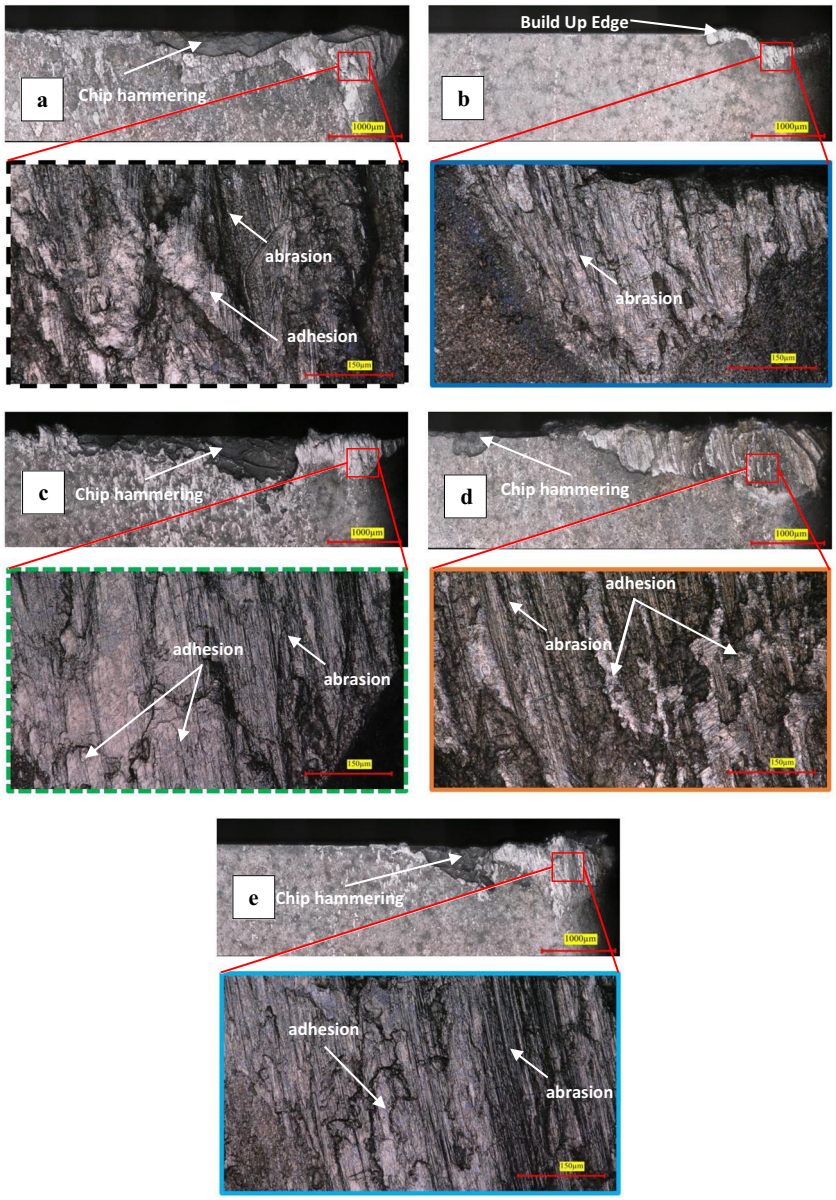

Fig. 15 Images of flank wear: **a** dry, **b** HPC, **c** MQL, **d** LN_2, and **e** flood ($a_p = 1.2$ mm, $V_c = 120$ m/min)

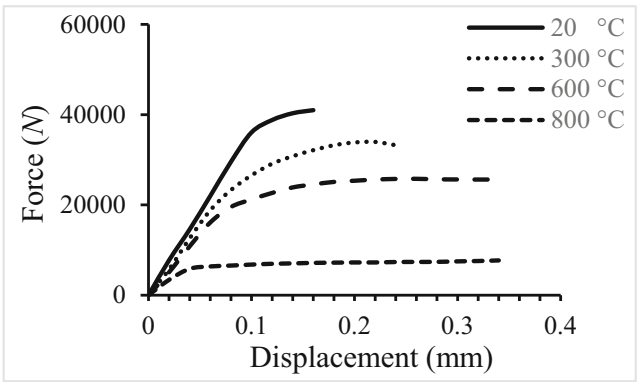

Fig. 16 The effects of temperature on deformation response of Ti-5553 alloy adapted from Germain et all [39]

and last pass is recorded in MQL conditions, while the smallest variation is recorded in HPC conditions. Frictional conditions also confirm that HPC provides much improved machining performance compared to other conditions presented here. Liquid nitrogen also makes a significant contribution to reduce the coefficient of friction compared with MQL, dry, and flood cooling conditions. Furthermore, the variation of frictional condition shows good agreement with the variation of tool wear in all machining conditions.

3.4 Chip morphology

The chip morphology of Ti-5553 alloy is also examined. The morphology of chips generated during machining tests at the

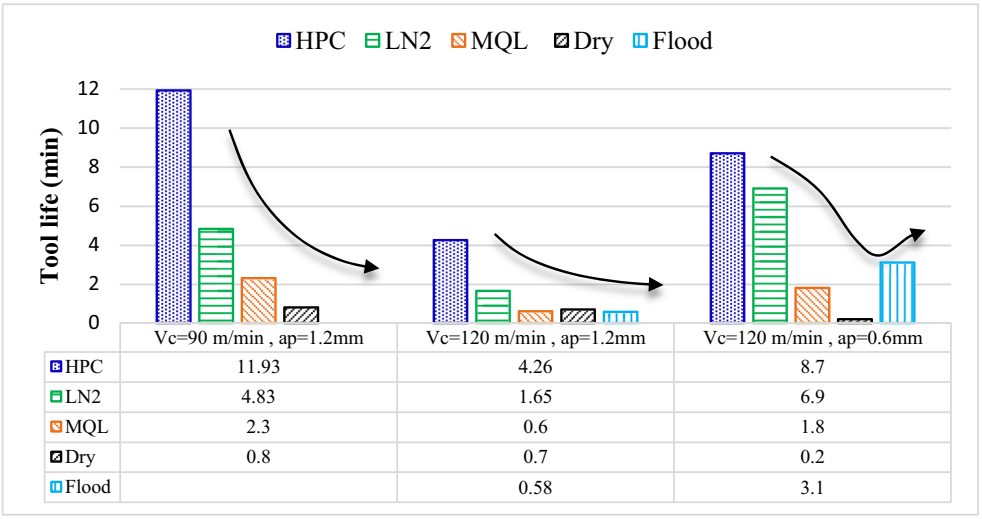

	Vc=90 m/min , ap=1.2mm	Vc=120 m/min , ap=1.2mm	Vc=120 m/min , ap=0.6mm
HPC	11.93	4.26	8.7
LN2	4.83	1.65	6.9
MQL	2.3	0.6	1.8
Dry	0.8	0.7	0.2
Flood		0.58	3.1

Fig. 17 Tool life under various machining conditions

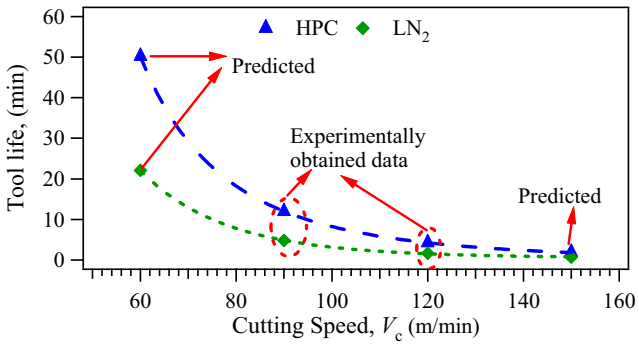

Fig. 18 Experimentally measured and calculated tool life under HPC machining conditions

first and last pass of the machining process of this alloy is presented in Fig. 21. The chips generated at the first pass can be considered as chips obtained from the machining process of this alloy with a fresh cutting tool. Similarly, the last pass indicates chips obtained by using a worn cutting tool. It is apparent that segmented chips were generated under all conditions at the first and last passes. Indeed, segmented chips are the typical chips produced when machining Ti alloys [43]. Chips were compared considering their thickness and shear angle to present quantitative data, as depicted in Fig. 22. In all a conditions, considerable difference in terms of chip morphology at the first and last pass is observed. In all conditions, thinner chips were obtained at the last pass when compared to the thickness of chips at the first pass, as shown in Fig. 23, indicating that a worn tool reduces the thickness of chips resulting from increased shear angle. A 22% reduction in thickness of chip is recorded in flood condition from the first pass to last pass, while it was 5.5% in MQL condition and approximately 7% in HPC condition. It should be also noted that high-pressure coolant reduces tool-chip contact length and consequently thinner chips obtained comparing with other conditions. Last pass results in much larger shear angles when comparing with the first pass in all conditions except for dry cutting. For instance while shear angle was 35° after first pass, it was measured as 43° after the last pass in cryogenic

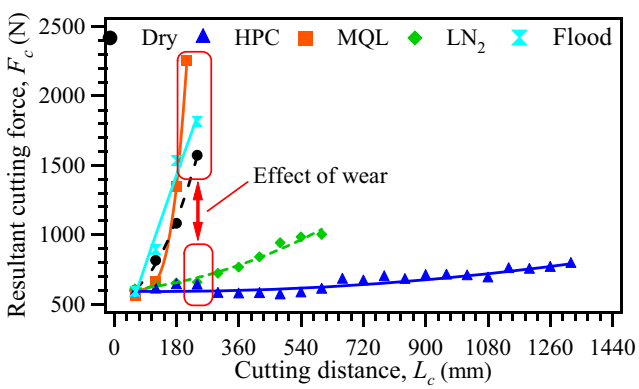

Fig. 19 Resultant fore under various machining conditions (V_c = 120 m/min, a_p = 1.2 mm)

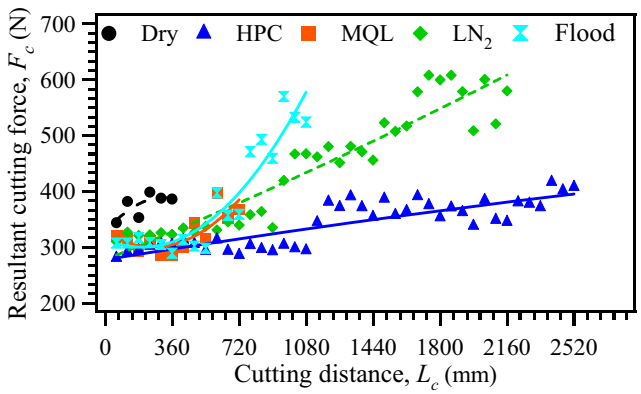

Fig. 20 Resultant fore under various machining conditions (V_c = 120 m/min, a_p = 0.6 mm)

Table 3 Variation of friction coeficient (μ) under as a function of machining conditions and cutting length ($V_c = 120$ m/min; $a_p = 1.2$ mm)

	First pass	Last pass	Percentage change (%)
Dry	0.54	2.52	367
Flood	0.55	2.49	353
MQL	0.53	2.79	426
LN_2	0.58	1.44	148
HPC	0.54	0.81	50

machining. Similarly, shear angles were 42.6° and 55° at the first and last passes in HPC condition, respectively (Fig. 24).

As a result of cutting process, extremely high deformation occurs on the chips at the shear band region, as depicted in Fig. 25. Grain refinement in the shear band is apparent under optical microscopy.

Compared to the first pass, very severe and extreme refinement and much thicker width of the shear band are observed, which indicate that at the lass pass chips were subject to very severe frictional conditions. The considerable difference between the first and the last pass in terms of the coefficient of friction presented in Table 3 explains the reason for obtaining chips that have much ticker width of shear bands. Consequently, it is possible to reach the conclusion that increased coefficient of friction resulting from the progression of tool wear also affects morphology of generated chips during the machining of near-beta titanium alloys.

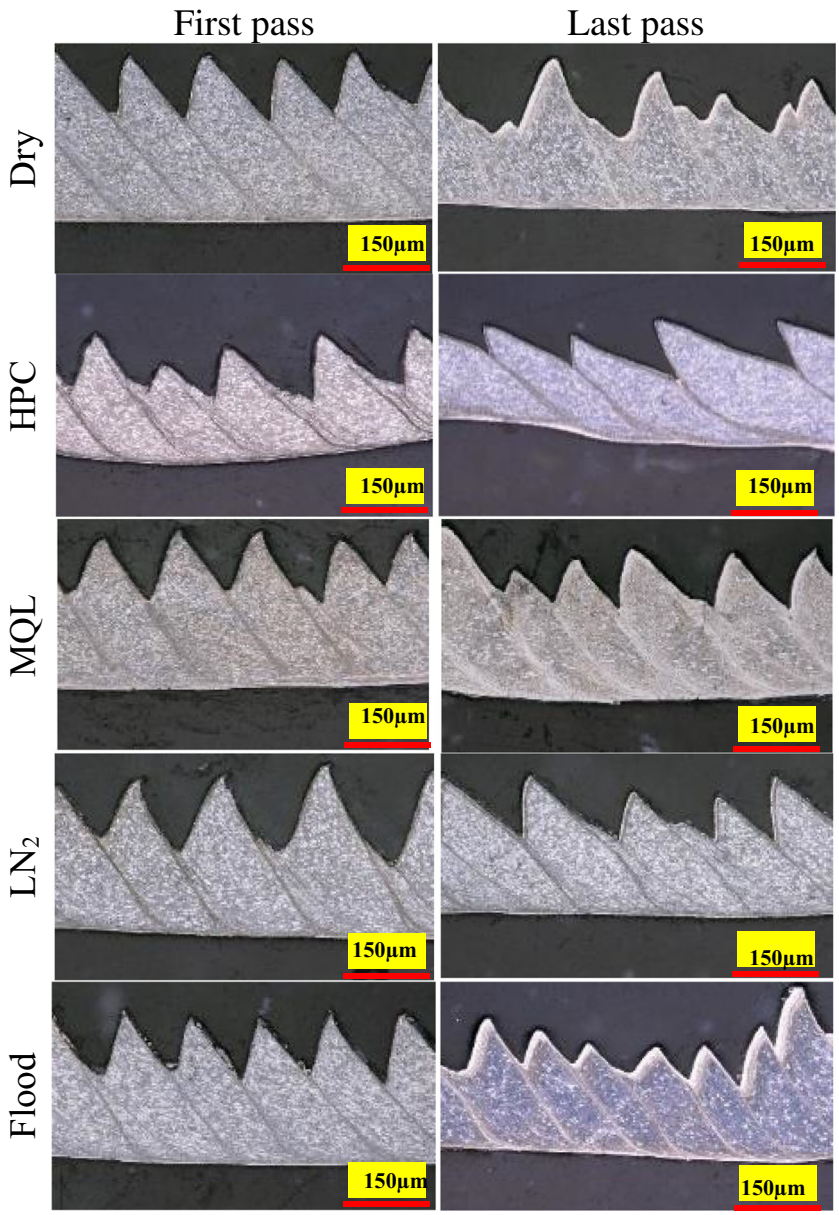

Fig. 21 Produced chips under various machining conditions ($a_p = 1.2$ mm, $V_c = 120$ m/min)

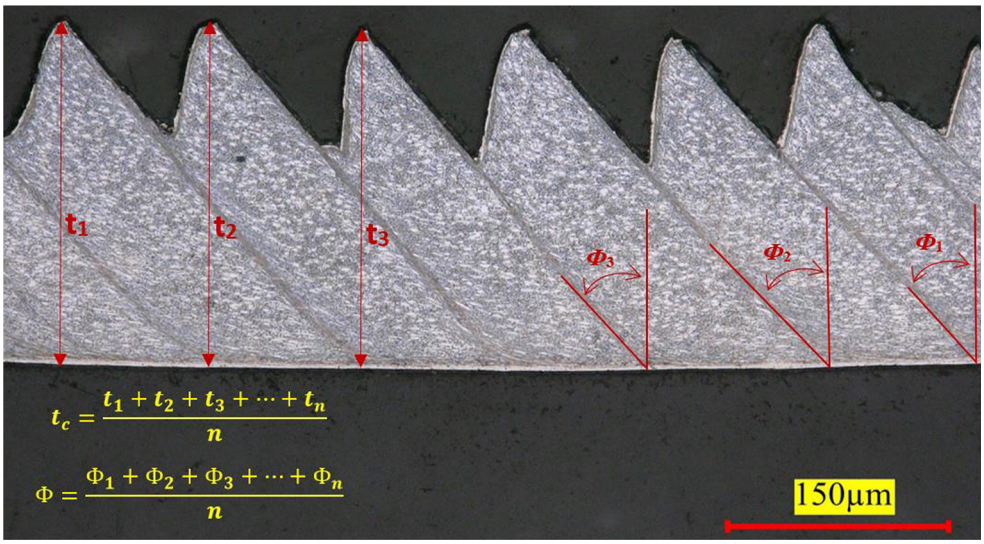

Fig. 22 Produced chips and measurement (dry, $a_p = 1.2$ mm, $V_c = 120$ m/min)

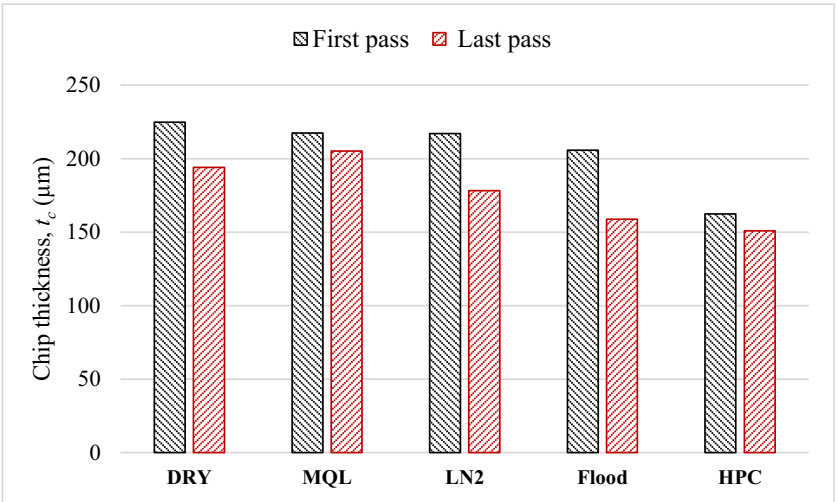

Fig. 23 Thickness of the produced chips under various machining conditions ($a_p =$ 1.2 mm, $V_c = 120$ m/min)

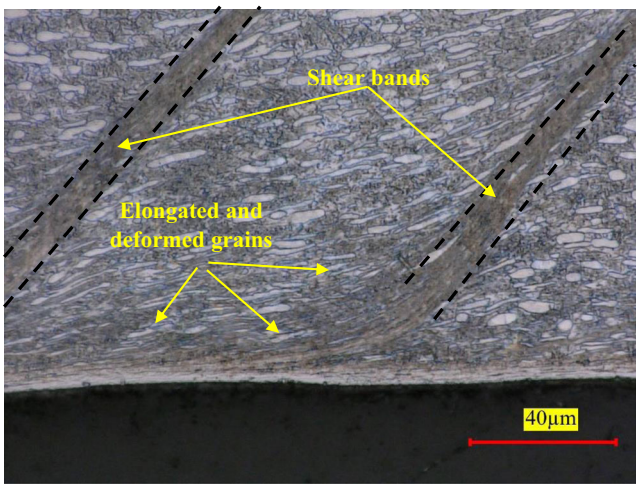

Fig. 24 Microstructure of the chip under various machining conditions ($a_p = 1.2$ mm, $V_c = 120$ m/min)

4 Conclusion

Near-beta titanium alloys, including Ti-5553 alloy are shown great interest by aerospace industries. However, these alloys are considered to be difficult-to-machine materials. Furthermore, very limited study in the literature focuses on understanding the chip formation process of this material. This study focuses on the progressive tool wear, tool life and corresponding cutting forces, frictional condition, cutting temperature, and chip morphology in the high speed machining process of near-beta titanium alloy under various cooling and lubrication conditions. To the best of the authors' knowledge, tool life in the machining of Ti-5553 alloy under various cooling and lubrication conditions presented for the first time in this study. Obtained results can be summarized as the follows:

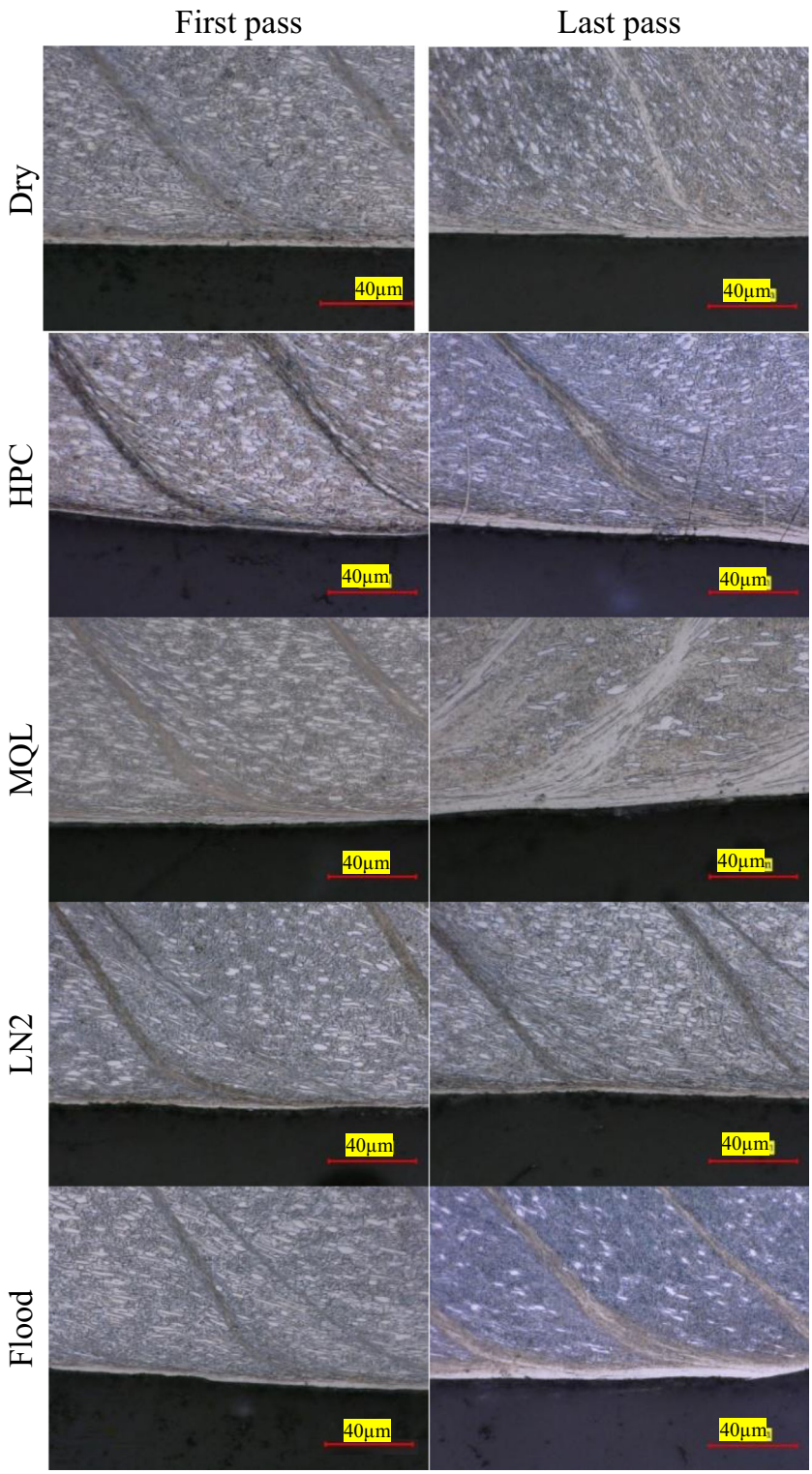

Fig. 25 Produced chips under various machining conditions (a_p = 1.2 mm, V_c = 120 m/min)

- Selecting high-pressure coolant improves cutting tool performance and increases tool life up to 12 min at 90 m/min cutting speed.
- Depth of cut plays a crucial role in the effectiveness of cooling and lubrication and consequently determines the tool life in the machining of Ti-5553 alloy.
- Cryogenic cooling is much more effective in smaller depth of cut (finish machining) compared to larger depth of cut in terms of tool life.
- Lower coefficient of friction and lower force components were recorded in the high-pressure cooling process when compared to other conditions.

– Chip morphology is induced from machining length and tool wear.

At high-speed cutting conditions, in particular 90 m/min and beyond, use of high-pressure coolant offers the best performance to increase tool life and to reduce, chip breaking, and energy consumption among all conditions tested here.

Acknowledgments The authors thank TUBITAK (The Scientific and Technological Research Council of Turkey) for supporting this work under project number 214M068.

References

1. Ezugwu E, Wang Z (1997) Titanium alloys and their machinability—a review. J Mater Process Technol 68:262–274
2. Sun S, Brandt M, Dargusch M (2009) Characteristics of cutting forces and chip formation in machining of titanium alloys. Int J Mach Tools Manuf 49:561–568
3. Schulze V, Zanger F (2011) Development of a simulation model to investigate tool wear in Ti-6Al-4V alloy machining. In: Advanced Materials Research, Trans Tech Publ, pp 535–544
4. Ezugwu E, Bonney J, Yamane Y (2003) An overview of the machinability of aeroengine alloys. J Mater Process Technol 134:233–253
5. Hughes J, Sharman A, Ridgway K (2006) The effect of cutting tool material and edge geometry on tool life and workpiece surface integrity. Proc Inst Mech Eng B J Eng Manuf 220:93–107
6. Venugopal K, Paul S, Chattopadhyay A (2007) Growth of tool wear in turning of Ti-6Al-4V alloy under cryogenic cooling. Wear 262: 1071–1078
7. Che-Haron C (2001) Tool life and surface integrity in turning titanium alloy. J Mater Process Technol 118:231–237
8. Veiga C, Davim J, Loureiro A (2013) Review on machinability of titanium alloys: the process perspective. Rev Adv Mater Sci 34: 148–164
9. Bermingham M, Kirsch J, Sun S, Palanisamy S, Dargusch M (2011) New observations on tool life, cutting forces and chip morphology in cryogenic machining Ti-6Al-4V. Int J Mach Tools Manuf 51:500–511
10. Ezugwu E (2004) High speed machining of aero-engine alloys. J Braz Soc Mech Sci Eng 26:1–11
11. Sun S, Brandt M, Dargusch M (2010) Thermally enhanced machining of hard-to-machine materials—a review. Int J Mach Tools Manuf 50:663–680
12. Rahman M, Wang Z-G, Wong Y-S (2006) A review on high-speed machining of titanium alloys. JSME Int J Ser C Mech Syst Mach Elem Manuf 49:11–20
13. Kaynak Y (2014) Evaluation of machining performance in cryogenic machining of Inconel 718 and comparison with dry and MQL machining. Int J Adv Manuf Technol 72(5–8):919–933
14. Kaynak Y, Lu T, Jawahir I (2014) Cryogenic machining-induced surface integrity: a review and comparison with dry, MQL, and flood-cooled machining. Mach Sci Technol 18:149–198
15. Jawahir I, Attia H, Biermann D, Duflou J, Klocke F, Meyer D, Newman S, Pusavec F, Putz M, Rech J (2016) Cryogenic manufacturing processes. CIRP Ann Manuf Technol 65:713–736
16. Shokrani A, Dhokia V, Newman ST (2012) Environmentally conscious machining of difficult-to-machine materials with regard to cutting fluids. Int J Mach Tools Manuf 57:83–101
17. Bermingham M, Palanisamy S, Kent D, Dargusch M (2012) A comparison of cryogenic and high pressure emulsion cooling technologies on tool life and chip morphology in Ti–6Al–4V cutting. J Mater Process Technol 212:752–765
18. Shokrani A, Dhokia V, Newman ST (2018) Energy conscious cryogenic machining of Ti-6Al-4V titanium alloy. Proc Inst Mech Eng B J Eng Manuf 232(10):1690–1706
19. Courbon C, Pusavec F, Dumont F, Rech J, Kopac J (2013) Tribological behaviour of Ti6Al4V and Inconel718 under dry and cryogenic conditions—application to the context of machining with carbide tools. Tribol Int 66:72–82
20. Mia M, Dhar NR (2018) Effects of duplex jets high-pressure coolant on machining temperature and machinability of Ti-6Al-4V superalloy. J Mater Process Technol 252:688–696
21. Braham-Bouchnak T, Germain G, Morel A, Furet B (2015) Influence of high-pressure coolant assistance on the machinability of the titanium alloy Ti555-3. Mach Sci Technol 19:134–151
22. Sun Y, Huang B, Puleo D, Jawahir I (2015) Enhanced machinability of Ti-5553 alloy from cryogenic machining: comparison with MQL and flood-cooled machining and modeling. Procedia CIRP 31:477–482
23. Kaynak Y, Gharibi A, Ozkutuk M (2018) Experimental and numerical study of chip formation in orthogonal cutting of Ti-5553 alloy: the influence of cryogenic, MQL, and high pressure coolant supply. Int J Adv Manuf Technol 94:1411–1428
24. Kaynak Y, Gharibi A, Yılmaz U, Köklü U, Aslantaş K (2018) A comparison of flood cooling, minimum quantity lubrication and high pressure coolant on machining and surface integrity of titanium Ti-5553 alloy. J Manuf Process 34:503–512
25. Baili M, Wagner V, Dessein G, Sallaberry J, Lallement D (2011) An experimental investigation of hot machining with induction to improve Ti-5553 machinability. In: Applied mechanics and Materials, Trans Tech Publ, pp 67–76
26. Wagner V, Baili M, Dessein G (2015) The relationship between the cutting speed, tool wear, and chip formation during Ti-5553 dry cutting. Int J Adv Manuf Technol 76:893–912
27. Huang C, Zhao Y, Xin S, Zhou W, Li Q, Zeng W (2017) Effect of microstructure on tensile properties of Ti–5Al–5Mo–5 V–3Cr–1Zr alloy. J Alloys Compd 693:582–591
28. Kar SK, Ghosh A, Fulzele N, Bhattacharjee A (2013) Quantitative microstructural characterization of a near beta Ti alloy, Ti-5553 under different processing conditions. Mater Charact 81:37–48
29. Nag S, Banerjee R, Srinivasan R, Hwang J, Harper M, Fraser H (2009) ω-Assisted nucleation and growth of α precipitates in the Ti–5Al–5Mo–5 V–3Cr–0.5 Fe β titanium alloy. Acta Mater 57: 2136–2147
30. Sun S, Brandt M, Palanisamy S, Dargusch MS (2015) Effect of cryogenic compressed air on the evolution of cutting force and tool wear during machining of Ti–6Al–4V alloy. J Mater Process Technol 221:243–254
31. Wang S, Nates R, Pasang T, Ramezani M (2015) Modelling of gas tungsten arc welding pool under Marangoni convection. Univ J Mech Eng 3:185–201
32. Campbell FC Jr (2011) Manufacturing technology for aerospace structural materials. Elsevier
33. Shokrani A, Dhokia V, Muñoz-Escalona P, Newman ST (2013). State-of-the-art cryogenic machining and processing. Int J Comput Integr Manuf 26(7):616–648
34. Dhananchezian M, Pradeep Kumar M (2011) Cryogenic turning of the Ti–6Al–4V alloy with modified cutting tool inserts. Cryogenics 51:34–40
35. Groover MP (2007) Fundamentals of modern manufacturing: materials processes, and systems. John Wiley & Sons

36. Ezugwu EO (2005) Key improvements in the machining of difficult-to-cut aerospace superalloys. Int J Mach Tool Manu 45: 1353–1367
37. Kaynak Y, Karaca HE, Noebe RD, Jawahir IS (2013) Tool-wear analysis in cryogenic machining of NiTi shape memory alloys: a comparison of tool-wear performance with dry and MQL machining. Wear 306:51–63
38. Stephenson D, Skerlos SJ, King AS, Supekar SD (2014) Rough turning Inconel 750 with supercritical CO2-based minimum quantity lubrication. J Mater Process Technol 214:673–680
39. Germain G, Morel A, Braham-Bouchnak T (2013) Identification of material constitutive laws representative of machining conditions for two titanium alloys: Ti6Al4V and Ti555-3. J Eng Mater Technol 135:031002
40. Baili M, Wagner V, Dessein G, Sallaberry J, Lallement D (2011) An experimental investigation of hot machining with induction to improve Ti-5553 machinability. Appl Mech Mater 62:67–76
41. Stephenson DA, Agapiou JS (1997) Metal cutting theory and practice. Marcel Dekker, INC, New York, pp 577–611
42. Bakkal M, Shih AJ, Scattergood RO (2004) Chip formation, cutting forces, and tool wear in turning of Zr-based bulk metallic glass. Int J Mach Tools Manuf 44:915–925
43. Sun S, Brandt M, Dargusch MS (2017) Effect of tool wear on chip formation during dry machining of Ti-6Al-4V alloy, part 1: effect of gradual tool wear evolution. Proc Inst Mech Eng B J Eng Manuf 231:1559–1574